Photoswitchable Magnetic Films: Prussian Blue Intercalated in Langmuir−Blodgett Films Consisting of an Amphiphilic Azobenzene and a Clay Mineral

ARTICLE *in* CHEMISTRY OF MATERIALS · MARCH 2004

Impact Factor: 8.35 · DOI: 10.1021/cm035223d

4 AUTHORS, INCLUDING:

Takashi Yamamoto
Keio University
24 PUBLICATIONS **334** CITATIONS

SEE PROFILE

Photoswitchable Magnetic Films: Prussian Blue Intercalated in Langmuir−Blodgett Films Consisting of an Amphiphilic Azobenzene and a Clay Mineral

Takashi Yamamoto,[†] Yasushi Umemura,[‡] Osamu Sato,[§] and Yasuaki Einaga*[,†]

Department of Chemistry, Faculty of Science and Technology, Keio University, 3-14-1 Hiyoshi, Yokohama 223-8522, Japan, Department of Applied Chemistry, National Defense Academy, 1-10-20 Hashirimizu, Yokosuka 239-8686, Japan, and Kanagawa Academy of Science and Technology, KSP, 3-2-1 Sakado, Kawasaki 213-0012, Japan

Received November 26, 2003. Revised Manuscript Received January 13, 2004

A novel photocontrollable magnetic thin film consisting of amphiphilic azobenzene cations, a smectite clay, and Prussian Blue has been designed and prepared by using the Langmuir−Blodgett method and an ion-exchange reaction. This magnetic thin film possesses a well-organized nanoscale layered structure. Reversible photoisomerization of the azobenzene chromophore realized photoswitching of the magnetization. The changes in the magnetization values were estimated to be ca. 11%. This figure was much larger than our previous system, which contained azobenzene multi-bilayered vesicles in a poly(vinyl alcohol) matrix (*J. Am. Chem. Soc.* **1999**, *121*, 3745). These larger changes in the magnetization values are due to the highly ordered structure of the hybrid multilayered films.

Introduction

Recently, photoresponsive materials have been a topic of great interest.[1−5] In particular, various kinds of photocontrollable materials have been reported in the field of magnetic materials.[6−8] However, there remain some limitations to the development of solid compounds such as these. To overcome these issues, we have focused on the incorporation of photochromic compounds, such as azobenzene and spiropyran, into magnetic systems to facilitate phototuning of the magnetization. This strategy has attracted much attention, and several kinds of photocontrollable magnets have been created by adopting this method.[9−15] In our previous work, we have reported on composite magnetic materials containing Prussian Blue intercalated into azobenzene multi-bilayered vesicles[9,10] and iron oxide particles enclosed by spiropyran vesicles.[11] However, the degree of photocontrol over the magnetization values was small in both cases. Therefore, it would be desirable to develop a novel photofunctional system that could achieve larger changes in the magnetization values by the use of photoillumination.

Ultrathin films with highly ordered structures have many applications in the field of optical devices, microelectronic devices, and sensors.[16−22] The Langmuir−Blodgett (LB) method is one of the most useful techniques for preparing thin films in which the number of layers and their sequence can be controlled at the molecular level.[16,17,23,24] This method is also effective in immobilizing functional groups on substrates, and a variety of deposition techniques have been reported.[25−32]

* Corresponding author. E-mail: einaga@chem.keio.ac.jp.
† Keio University.
‡ National Defense Academy.
§ Kanagawa Academy of Science and Technology.

(1) Advincula, R.; Park, M.-K.; Baba, A.; Kaneko, F. *Langmuir* **2003**, *19*, 654.
(2) Rosenbaum, T. F.; Hoekstra, F. T. *Adv. Mater.* **2002**, *14*, 247.
(3) Benkö, Gábor.; Kallioinen, J.; Korppi-Tommola, J. E. I.; Yartsev, A. P.; Sundström, V. *J. Am. Chem. Soc.* **2002**, *124*, 489.
(4) Advincula, R. C.; Fells, E.; Park, M.-K. *Chem. Mater.* **2001**, *13*, 2870.
(5) Lee, H.-K.; Kanazawa, A.; Shiono, T.; Ikeda, T. *J. Appl. Phys.* **1999**, *86*, 5927.
(6) Sato, O.; Iyoda, T.; Fujishima, A.; Hashimoto, K. *Science* **1996**, *272*, 704.
(7) Pejakovic, D. A.; Kitamura, C.; Miller, J. S.; Epstein, A. J. *Phys. Rev. Lett.* **2002**, *88*, 057202−1.
(8) Matsuda, K.; Irie, M. *J. Am. Chem. Soc.* **2001**, *123*, 9896.
(9) Einaga, Y.; Yamamoto, T.; Sugai, T.; Sato, O. *Chem. Mater.* **2002**, *14*, 4846.
(10) Einaga, Y.; Sato, O.; Iyoda, T.; Fujishima, A.; Hashimoto, K. *J. Am. Chem. Soc.* **1999**, *121*, 3745.
(11) Einaga, Y.; Taguchi, M.; Li, G.-M.; Akitsu, T.; Gu, Z.-Z.; Sugai, T.; Sato, O. *Chem. Mater.* **2003**, *15*, 8.
(12) Benard, S.; Leaustic, A.; Riviere, E.; Yu, P.; Clement, R. *Chem. Mater.* **2001**, *13*, 3709.
(13) Benard, S.; Riviere, E.; Yu, P.; Nakatani, K.; Delouis, J. F. *Chem. Mater.* **2001**, *13*, 159.
(14) Nakatani, K.; Yu, P. *Adv. Mater.* **2001**, *13*, 1411.
(15) Benard, S.; Yu, P. *Adv. Mater.* **2000**, *12*, 48.
(16) Ulman, A. *An Introduction to Ultrathin Organic Films: From Langmuir−Blodgett to Self-Assembly*; Academic Press: San Diego, CA, 1991.
(17) Petty, M. C. *Langmuir−Blodgett Films: An Introduction*; Cambridge University Press: Cambridge, U.K., 1996.
(18) Ulman, A. *Chem. Rev.* **1996**, *96*, 1533.
(19) Mallouk, T. E.; Gavin, J. A. *Acc. Chem. Res.* **1998**, *31*, 209.
(20) Okamoto, K.; Tamura, K.; Takahashi, M.; Yamagishi, A. *Colloids Surf. A* **2000**, *169*, 241.
(21) Liu, M.; Ushida, K.; Kira, A.; Nakahara, H. *J. Phys. Chem. B* **1997**, *101*, 1101.
(22) Rella, R.; Serra, A.; Siciliano, P.; Terope, A.; Valli, L.; Zocco, A. *Langmuir* **1997**, *13*, 6562.
(23) Kuhn, H.; Möbius, D.; Bücher, H. *In Physical Methods of Chemistry, Pt. IIIB*; Wiley-Interscience: New York, 1972; Chapter VII.
(24) Gaines, G. L., Jr. *In Insoluble Monolayers at Liquid−Gas Interfaces*; Wiley-Interscience: New York, 1966.
(25) Umemura, Y. *J. Phys. Chem. B* **2002**, *106*, 11168.
(26) Umemura, Y.; Yamagishi, A.; Schoonheydt, R.; Persoons, A.; De Schryber, F. *J. Am. Chem. Soc.* **2002**, *124*, 992.
(27) Umemura, Y.; Yamagishi, A.; Schoonheydt, R.; Persoons, A.; De Schryber, F. *Langmuir* **2001**, *17*, 449.

10.1021/cm035223d CCC: $27.50
Published on Web 03/03/2004

One example of the implementation of these techniques is the use of a clay mineral.[25−27] When amphiphilic cations are spread onto an aqueous suspension of a clay mineral in a LB trough, negatively charged clay platelets in the suspension are adsorbed electrostatically onto the bottom of a floating monolayer of cations at the air−suspension interface. Hybrid monolayers of clay platelets and amphiphilic cations formed in this way can be deposited onto a solid surface by horizontal dipping. The outer surface of the transferred film is covered with a clay layer, and some exchangeable cations remain on the outer surface of the clay layer unless the negative charge of the clay layer is neutralized completely by the positive charge of the amphiphilic cations. Thus, the metal cations, such as Na^+, remaining on the outer surface are ion-exchangeable. When the outer surface of the film is dipped in a solution of a cationic compound, the cationic compound is adsorbed on the surface by an ion-exchange reaction to form a layer of cations. By repeating these procedures, we can prepare hybrid multilayered films consisting of amphiphilic cations, clay platelets, and the adsorbed cations.

For the work reported herein, we have designed a novel type of hybrid multilayered films consisting of amphiphilic azobenzene cations (a photochromic compound), a smectite clay (montmorillonite; Kunipia P), and Prussian Blue (a ferromagnet at low temperature). By using this photofunctional system, larger photoinduced changes in the magnetization values are expected to be realize due to the highly ordered molecular orientation of the LB film. The properties of the hybrid multilayered films were confirmed by surface pressure−molecular area ($\pi-A$) isotherm measurements, UV−vis spectroscopy (UV−vis), infrared−external reflection spectroscopy (IR−ER), X-ray diffraction (XRD), and magnetization measurements (SQUID).

Experimental Section

Materials. The hybrid multilayered film was composed of an azobenzene derivative {5-[4-(4-dodecyloxyphenylazo)phenoxy]pentyl}(2-hydroxyethyl)dimethylammonium bromide (=C_{12}-$AzoC_5N^+$) as the amphiphilic cation, montmorillonite (Kunipia P) as the clay mineral, and Prussian Blue (PB) as the magnetic material. $C_{12}AzoC_5N^+$ was synthesized according to a previous report.[33] $C_{12}AzoC_5N^+$ was dissolved in a 9:1 mixture (by volume) of dichloromethane and ethanol to prepare a solution at 2.7×10^{-3} M.

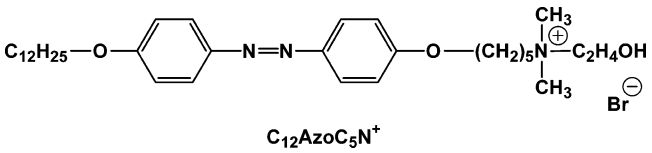

$C_{12}AzoC_5N^+$

The smectite clay mineral that we used (montmorillonite) was Kunipia P from Kunimine Co., Japan. The cation-exchange capacity (CEC) of the clay was 1.074 mequiv g^{-1}. The thickness of the clay platelets, estimated from their crystal structure, was 0.96 nm.[34−36] The stock suspension of the clay was prepared by dispersing 1 g of the clay in 1000 mL of pure water and diluting it to a given concentration with pure water just before it was used as a subphase.

$FeCl_2 \cdot 4H_2O$ and $K_3[Fe(CN)_6]$ were purchased from WAKO Pure Chemicals and used without further purification. The water was purified with a Simpli Lab water system (Millipore) to a specific resistivity of 18.2 MΩ cm.

Substrate Preparation. Glass plates were used as deposition substrates for the UV−vis, IR−ER, and XRD measurements. The samples for SQUID measurement were prepared on a micro-cover-glass (thickness 0.12−0.17 mm) and all of the substrates were rendered hydrophobic by treating them with octadecyltriethoxysilane.

Film Preparation. A schematic illustration of the film preparation process is shown in Figure 1. The solution of C_{12}-$AzoC_5N^+$ was spread on a subphase of the clay suspension (50 ppm) at room temperature. A floating monolayer of C_{12}-$AzoC_5N^+$ was hybridized with the clay platelets at the air−suspension interface. Fifteen minutes later, the floating hybrid monolayers were compressed with a surface pressure of 30 mN m^{-1}. After 30 min, the floating hybrid monolayers were transferred as X-type films onto the hydrophobic surface of the glass substrates by a horizontal dipping technique.[27,37,38] The surface of the transferred film was rinsed with pure water several times, and was then immersed in an aqueous $FeCl_2$ solution (1 mM) for 1 min to exchange the Fe ions with the exchangeable metal ions. After rinsing the surface well with pure water, it was dipped in an aqueous $K_3[Fe(CN)_6]$ solution (1 mM) for 1 min to form a PB layer on the surface of the hybrid film. The surface was rinsed well with pure water and dried by blasting with N_2. The hybrid multilayered films composed of $C_{12}AzoC_5N^+$, clay platelets, and PB were fabricated by repeating this method. One unit layer composed of $C_{12}AzoC_5N^+$, the clay platelets, and PB is hereafter designated as one hybrid layer.

Instruments. The preparation of the floating hybrid monolayer and measurements of the surface pressure−molecular area ($\pi-A$) isotherms were carried out using a computer-controlled film balance system (FSD-50, USI System, Japan). UV−visible absorption spectra were recorded on a V-560 spectrophotometer (JASCO). UV−vis measurement at low temperature was performed with a closed-cycle helium refrigerator (Iwatani. Co., Ltd.). UV illumination (filtered light, λ_{max} = 360 nm, 1.0 mW cm^{-2}) was carried out using an ultra-high-pressure mercury lamp (HYPERCURE 200, Yamashita Denso). Similarly, visible light illumination (400−700 nm, 1 mW cm^{-2}) was carried out using a xenon lamp (XFL-300, Yamashita Denso). Infrared external reflection absorption spectra were recorded on a Spectrum One FT-IR spectrometer (Perkin-Elmer Japan) equipped with a variable angle specular reflectance accessory. The X-ray diffraction (XRD) patterns were recorded on a Philips X′Pert MRD high-resolution X-ray diffractometer using Ni-filtered Cu Kα radiation. The magnetic properties were investigated with a superconducting quantum interface device (SQUID) magnetometer (model MPMS-5S, Quantum Design).

Results and Discussion

***π*−*A* Isotherms of the Floating Hybrid Monolayers on Clay Suspensions.** Figure 2 shows the $\pi-A$

(28) Tachibana, H.; Yamanaka, Y.; Sakai, H.; Abe, M.; Matsumoto, M. *Colloids Surf. A* **2002**, *198−200*, 83.
(29) Kawai, T. *J. Phys. Chem. B* **1999**, *103*, 5517.
(30) Ha, K.-R.; Kim, J.-M.; Rabolt, J. F. *Thin Solid Films* **1999**, *347*, 272.
(31) Lafuente, C.; Mingotaud, C.; Delhaes, P. *Chem. Phys. Lett.* **1999**, *302*, 523.
(32) Mingotaud, C.; Lafuente, C.; Amiell, J.; Delhaes, P. *Langmuir* **1999**, *15*, 289.
(33) Shimonura, M.; Ando, R.; Kunitake, T. *Ber. Bunsen-Ges. Phys. Chem.* **1983**, *87*, 1134.
(34) Theng, B. K. G. *The Chemistry of Clay-Organic Reactions*; Adam Hilger: London, 1974.
(35) Van Duffel, B.; Schoonheydt, R. A.; Grim, C. P. M.; De Schryver, F. C. *Langmuir* **1999**, *15*, 7520.
(36) Moore, D. M.; Reynolds, R. C., Jr. *X-ray Diffraction and the Identification and Analysis of Clay Minerals*; Oxford University Press: New York, 1997.
(37) Kawamata, J.; Ogata, Y.; Taniguchi, M.; Yamagishi, A.; Inoue, K. *Mol. Cryst. Liq. Cryst.* **2000**, *343*, 53.
(38) Umemura, Y.; Yamagishi, A.; Schoonheydt, R.; Persoons, A.; De Schryver, F. *Thin Solid Films* **2001**, *388*, 5.

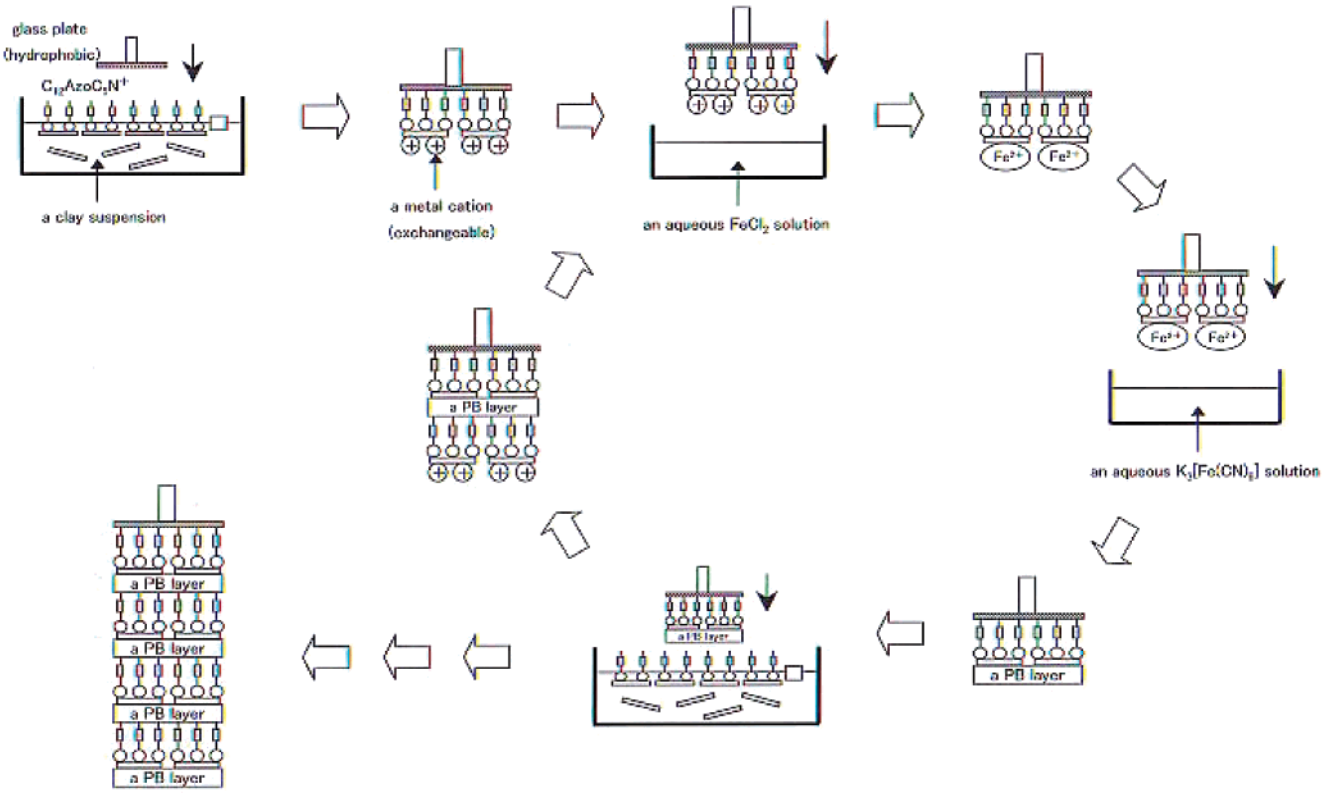

Figure 1. Preparation method of the hybrid multilayered films containing $C_{12}AzoC_5N^+$, the clay platelets, and PB.

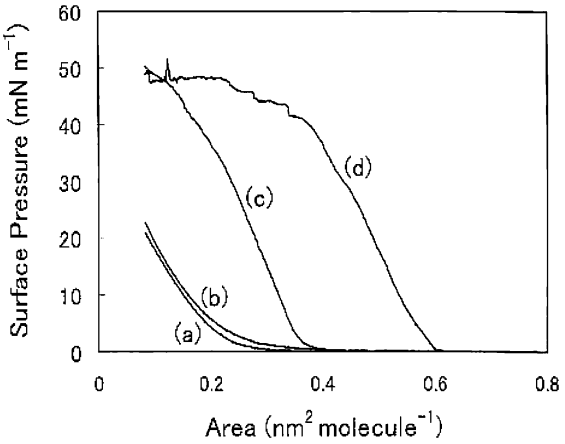

Figure 2. $\pi-A$ isotherm curves for floating monolayers of $C_{12}AzoC_5N^+$ on (a) pure water and on the clay suspensions at (b) 5, (c) 50, and (d) 100 ppm.

isotherms of the floating hybrid monolayers when a solution of $C_{12}AzoC_5N^+$ was spread onto the surface of the clay suspensions at 5, 50, and 100 ppm and also onto pure water. The $\pi-A$ isotherm of the floating hybrid monolayers on the clay suspension at 5 ppm (Figure 2b) was similar to that on pure water (Figure 2a). This indicates that the $C_{12}AzoC_5N^+$ dissolved in the subphase before interacting with the clay platelets. On the other hand, the $\pi-A$ isotherm of the floating hybrid monolayers on the clay suspension at 100 ppm (Figure 2d) lifted off at around 0.6 nm^2 molecule^{-1} with a surface pressure of 0 mN m^{-1}, and as the floating hybrid monolayers were compressed, the surface pressure increased up to 40 mN m^{-1}. At this point (0.4 nm^2 molecule^{-1}), the floating hybrid monolayers collapsed. Remarkably, the $\pi-A$ isotherm of the floating hybrid monolayers on the clay suspension at 50 ppm (Figure 2c) showed the formation of stable hybrid monolayers at the air−suspension interface and the surface pressure increased up to more than 40 mN m^{-1}.

The formation mechanism of the floating hybrid monolayers was reported previously.[38] Briefly, when the solution of $C_{12}AzoC_5N^+$ is spread onto the surface of the clay suspension, the clay platelets in the suspension are adsorbed electrostatically onto the bottom of the floating $C_{12}AzoC_5N^+$ monolayers. If the clay concentration is high, the adsorption rate of the clay platelets is high. In this case, cations of $C_{12}AzoC_5N^+$ are captured immediately by the clay platelets at the air−suspension interface before cations of $C_{12}AzoC_5N^+$ aggregate to form monolayer domains. As a result, $C_{12}AzoC_5N^+$ forms stable hybrid monolayers without dissolving in the subphase.

UV−Vis Absorption Spectra of the Hybrid Multilayered Films. UV−vis absorption spectra of the hybrid multilayered films measured at room temperature are shown in Figure 3. Each spectrum gave two intense absorption peaks at 370 nm and around 700 nm. The peak at 370 nm is ascribed to the $\pi-\pi^*$ transition of the trans isomer of $C_{12}AzoC_5N^+$ and the peak at around 700 nm is related to the intervalence charge transfer (IVCT) band from Fe^{II} to Fe^{III} in the PB layer. The absorption intensity increased with increasing numbers of hybrid layers. It is noteworthy that the IVCT band of PB was blue-shifted upon increasing the number of hybrid layers (inset of Figure 3). This spectral shift indicates the growth of PB domains in the hybrid multilayered films. At first, the PB domains were very small, probably existing as nanometer-sized islands. As the number of hybrid layers increased, these PB domains became linked with each other, wherein PB forms a sheetlike two-dimensional network. A similar result

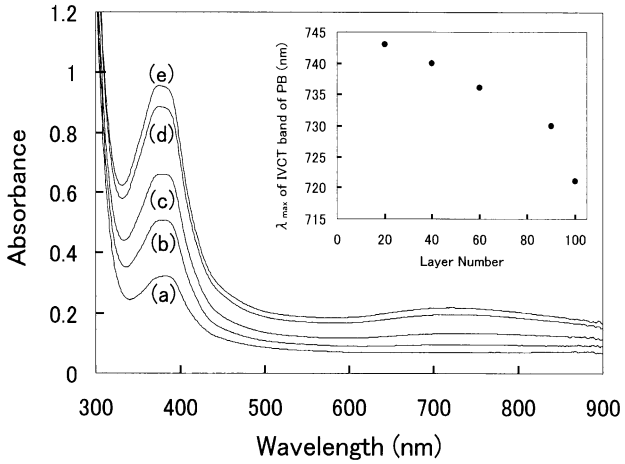

Figure 3. UV−vis absorption spectra for hybrid multilayered films [(a) 20, (b) 40, (c) 60, (d) 90, and (e) 100 hybrid layers]. The inset shows the relation between the λ_{max} of the IVCT band of PB and the number of hybrid layers.

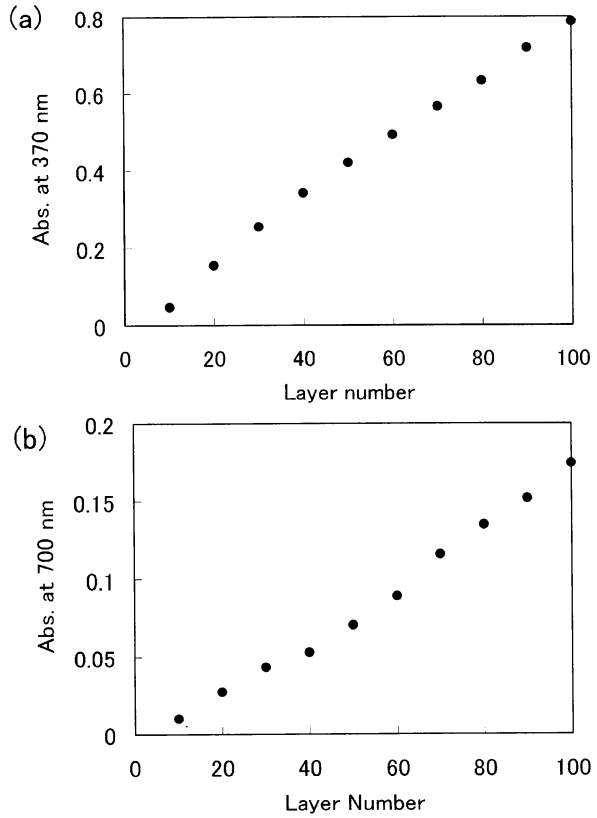

Figure 4. Changes in absorbance at (a) $\lambda = 370$ nm and (b) $\lambda = 700$ nm against the number of hybrid layers. Background subtraction was done for both data.

has been observed in self-assembled films of PB.[39] The absorbance at 370 and 700 nm was plotted in Figure 4a,b as a function of the number of hybrid layers. As seen in Figure 4a,b, the absorbance increased linearly as the number of hybrid layers increased. This indicates a reproducible transfer of the floating hybrid monolayers from one to the next.

Photoisomerization of the hybrid multilayered films was monitored by UV−vis absorption spectroscopy. The UV−vis spectral changes due to photoisomerization at

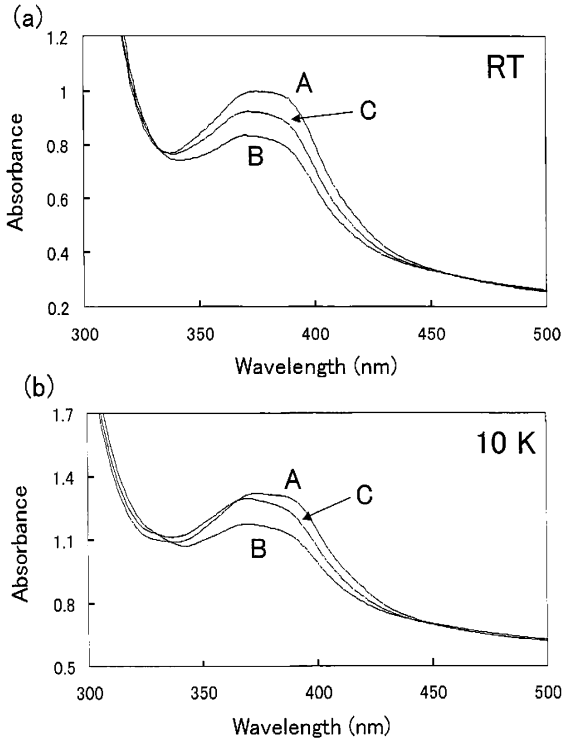

Figure 5. Changes in the optical absorption spectra for a 100-layer hybrid film due to photoisomerization (a) at room temperature and (b) at 10 K. In both spectra, the initial trans state (A) was first illuminated with UV light for 20 min (B). Then, it was subsequently illuminated with visible light for 20 min (C).

room temperature and at 10 K are shown in Figure 5. Before light illumination, the hybrid multilayered films only consisted of the trans form of $C_{12}AzoC_5N^+$, because it is thermodynamically more stable than the cis form.[40] At room temperature (Figure 5a), UV illumination of the trans-isomer resulted from the decrease of the absorbance at 370 nm, which is ascribed to the $\pi-\pi^*$ transitions of the trans-isomer. This indicates that trans-to-cis isomerization occurred in the hybrid multilayered films. Moreover, the fraction of cis-isomer at the photostationary state was estimated to be ca. 45% by using a calculation based on the difference spectra.[41] This is because the photoisomerization of azobenzene derivatives, particularly trans-to-cis isomerization, is accompanied by an increase in the molecular volume. In fact, it is known that isomerization proceeds to some extent in LB films,[42] and the quantum efficiency for photoisomerization is reduced from that in the organic solvent.[43] After subsequent illumination with visible light, the reverse process (i.e. cis-to-trans isomerization) also proceeded to a certain degree. The overall trans−cis isomerization cycle was repeated in the area from curve B to C several times by alternative illumination with UV and visible light. Similar results have been reported for other LB films that contain azobenzene

(39) Pyrasch, M.; Tieke, B. *Langmuir* **2001**, *17*, 7706.

(40) Adamson, A. A.; Volger, A.; Kunkely, H.; Wachter, R. *J. Am. Chem. Soc.* **1978**, *100*, 1298.

(41) Brode, W. R.; Gould, J. H.; Wyman, G. M. *J. Am. Chem. Soc.* **1952**, *74*, 4641.

(42) Nakahara, H.; Fukuda, K.; Shimomura, M.; Kunitake, T. *Nippon Kagaku Kaishi* **1988**, *7*, 1001.

(43) Schönhoff, M.; Mertesdorf, M.; Lösche, M. *J. Phys. Chem.* **1996**, *100*, 7558.

derivatives.[44−46]

Subsequently, UV−vis spectral measurements were carried out at 10 K using a closed-cycle helium refrigerator. Even at low temperature, cis−trans isomerization was also observed (Figure 5b) and the photoisomerization was repeated in the area from curve B to C several times by alternating light illumination. Moreover, this is almost consistent with the changes in the absorption spectra at room temperature (i.e. the area from curve B to C in Figure 5a).

Structures of the Hybrid Multilayered Films. To get information on the orientation of the alkyl chains of $C_{12}AzoC_5N^+$ in the hybrid multilayered films, p-polarized IR−ER spectra were measured. In p-polarized IR−ER spectra, a surface-normal transition moment appears as a positive band, while a surface-tangential one appears as a negative band when the angle of incidence is smaller than the Brewster angle [$\theta_B = \tan^{-1}(n_{subst}/n_{air}) = 56°$ (for a glass); n_{subst} and n_{air} are refractive indices of the substrate and air, respectively]. Above θ_B, however, the sign of the bands changes oppositely.[47,48] Thus, the direction of the transition moment can be estimated from the p-polarized IR−ER spectral data obtained at the various incident angles.

Figure 6a shows p-polarized IR−ER spectra in the $-CH_2-$ stretching vibration region for the hybrid multilayered films measured at the various incident angles. These spectra give two absorption peaks at 2914 and 2847 cm^{-1}, which are assigned to the antisymmetric and symmetric $-CH_2-$ stretching [$\nu_a(CH_2)$ and $\nu_s(CH_2)$] vibrations of $C_{12}AzoC_5N^+$, respectively. The reflection absorbance for the $\nu_a(CH_2)$ and $\nu_s(CH_2)$ bands was plotted in Figure 6b as a function of the incident angle. As can be seen in Figure 6a,b, the peaks due to both bands appear as the negative absorbance below θ_B and, on the other hand, the same peaks appear as the positive one in the spectra with the incident angle above θ_B. These spectral data indicate that the transition moments of the $\nu_a(CH_2)$ and $\nu_s(CH_2)$ bands are estimated to be parallel to the film surface; that is, the alkyl chain of $C_{12}AzoC_5N^+$ in the hybrid multilayered films are almost perpendicular to the layers.

The XRD pattern for the hybrid multilayered films (100 hybrid layers) gave six diffraction peaks at $2\theta = 2.70°$, 6.18°, 9.82°, 14.1°, 17.6°, and 22.1° (Figure 7). The diffraction peaks observed at $2\theta = 2.70°$, 6.18°, 9.82°, 14.1°, and 22.1° correspond to the (001), (002), (003), (004), and (005) reflections of the clay layer. This indicates that the hybrid film possesses a layered structure. In addition, the thickness of one hybrid layer ($C_{12}AzoC_5N^+$/clay/PB) is calculated to be 3.27 nm. Considering that the thickness of a clay platelet is 0.96 nm,[34−36] the total thickness of the $C_{12}AzoC_5N^+$ and PB layers should therefore be 2.31 nm. To determine the precise structure of the adsorbed PB layer, it is essential to confirm the molecular orientation of $C_{12}AzoC_5N^+$. According to the single-crystal X-ray structure analysis of $C_{12}AzoC_5N^+$,[49] the molecular length of $C_{12}AzoC_5N^+$ has been determined to be 1.71 nm. As mentioned above, the orientation of $C_{12}AzoC_5N^+$ is perpendicular to the film surface, and therefore, the layer thickness of $C_{12}AzoC_5N^+$ is estimated to be 1.71 nm. From these

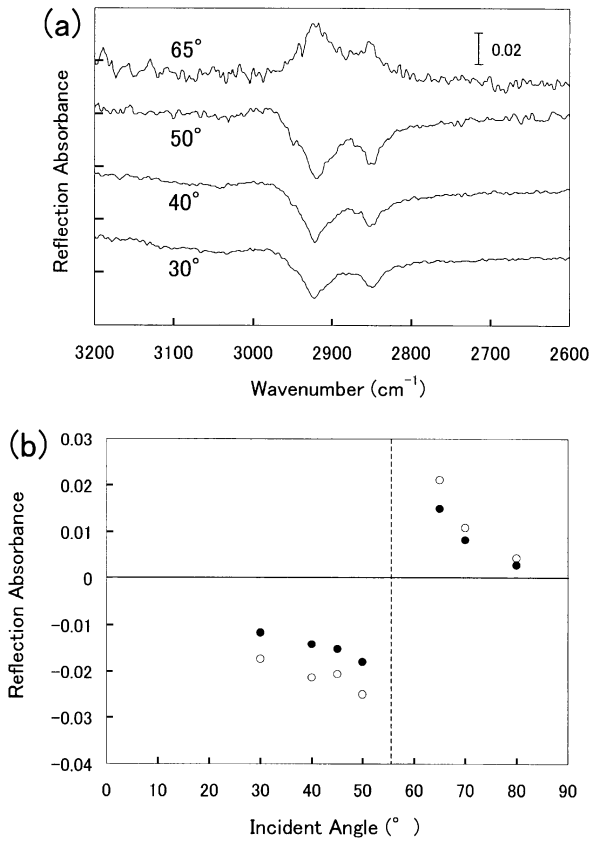

Figure 6. (a) p-Polarized IR−ER spectra in the $-CH_2-$ stretching vibration region of a 50-layer hybrid film at incident angles of 30°, 40°, 50°, and 65°. (b) Relation between reflection absorbance and the incident angle. The open and solid circles are reflection absorbance for the $\nu_a(CH_2)$ and $\nu_s(CH_2)$ bands, respectively.

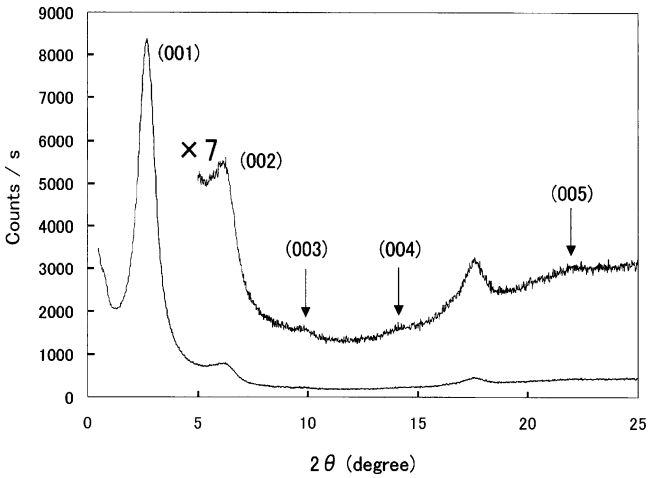

Figure 7. X-ray diffraction pattern for a 100-layer hybrid film.

(44) Tachibana, H.; Yamada, T.; Sakai, H.; Abe, M.; Matsumoto, M. *Mol. Cryst. Liq. Cryst.* **2000**, *345*, 119.
(45) Matsumoto, M.; Miyazaki, D.; Tanaka, M.; Azumi, R.; Manda, E.; Kondo, Y.; Yoshino, N.; Tachibana, H. *J. Am. Chem. Soc.* **1998**, *120*, 1479.
(46) Tachibana, H.; Azumi, R.; Tanaka, M.; Matsumoto, M.; Sako, S.; Sakai, H.; Abe, M.; Kondo, Y.; Yoshino, N. *Thin Solid Films* **1996**, *284*, 73.
(47) Hasegawa, T.; Umemura, J.; Takenaka, T. *J. Phys. Chem.* **1993**, *97*, 9009.
(48) Hasegawa, T.; Nishijo, J.; Umemura, J.; Theiss, W. *J. Phys. Chem. B* **2001**, *105*, 11178.
(49) Okuyama, K.; Watanabe, H.; Shimonura, M.; Hirabayashi, K.; Kunitake, T.; Kajiyama, T.; Yasuoka, N. *Bull. Chem. Soc. Jpn.* **1986**, *59*, 3351.

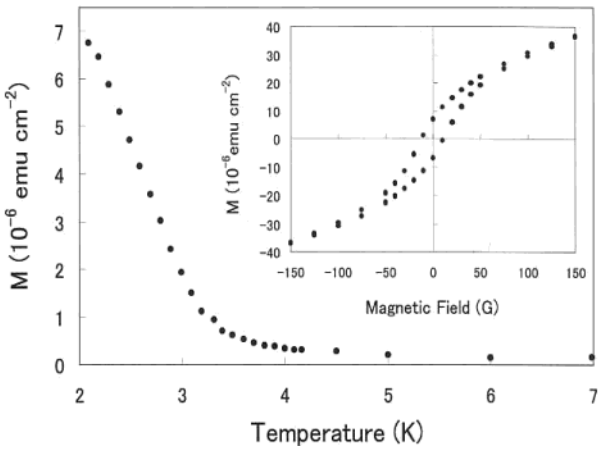

Figure 8. Field-cooled magnetization curve with an external magnetic field of 10 G for a 24-layer hybrid film. This film exhibits ferromagnetic properties with a critical temperature of $T_c = 3.2$ K. The inset shows a hysteresis loop for a 24-layer hybrid film at 2 K.

estimations, the thickness of the adsorbed PB layers (−CN−Fe^{III}−NC−Fe^{II}−O) is determined to be 0.60 nm. On this occasion, we suggest that roughly one layer of the three-dimensional PB network is formed, even in the hybrid multilayered films.

Magnetic Properties of the Hybrid Multilayered Films. The field-cooled magnetization curve at an external magnetic field of 10 G for the hybrid multilayered films exhibits ferromagnetic properties with a critical temperature (T_c) of 3.2 K (Figure 8). This lower T_c value than that of the bulk PB (5.6 K)[50] indicates that the number of exchange pathways per magnetic ion is reduced due to lowering structural coherence or the dimensions. This was consistent with the structure estimated by XRD, i.e., that PB layers are intercalated into the hybrid films. In addition, the presence of a ferromagnetic interaction at low temperature was supported by the plot of the magnetization as a function of an external magnetic field at 2 K, where a magnetic hysteresis loop was observed with a coercive field of 10 G and a remnant magnetization of 7.07×10^{-6} emu cm^{-2}. This tendency also exhibits a ferromagnetic trend (inset of Figure 8).

Subsequently, we observed the influence of light illumination on the magnetic properties of the hybrid multilayered films and also determined how the magnetization changed by alternate illumination with UV and visible light at 2 K (Figure 9). During the UV light illumination (360 nm, 1.0 mw cm^{-2}, 25 min), the magnetization value decreased from 6.72×10^{-6} to 6.07×10^{-6} emu cm^{-2}. Even after the light illumination was stopped, this decreased magnetization value was maintained for at least 2 h. Then, we illuminated the films with visible light (400−700 nm, 1.0 mW cm^{-2}) for a further 10 min. The magnetization value recovered by ca. 55% (to ca. 6.42×10^{-6} emu cm^{-2}). After this process, the UV-light-induced decrease and the visible-light-induced increase of the magnetization were repeated several times. The total photoinduced changes in the magnetization values are estimated to be ca. 11%.

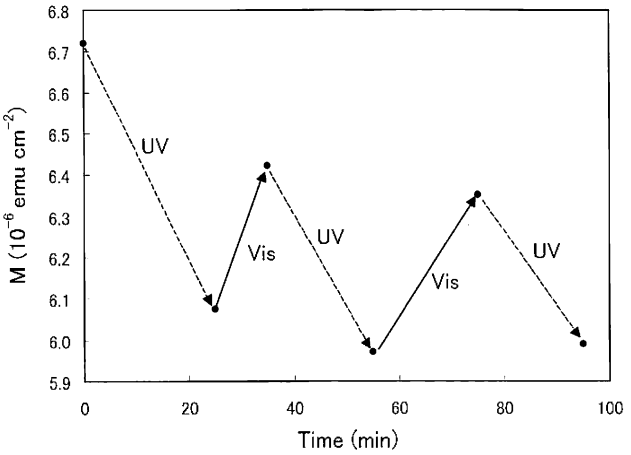

Figure 9. Changes in the magnetization for a 24-layer hybrid film, induced by UV and visible light illumination at 2 K with an external magnetic field of 10 G.

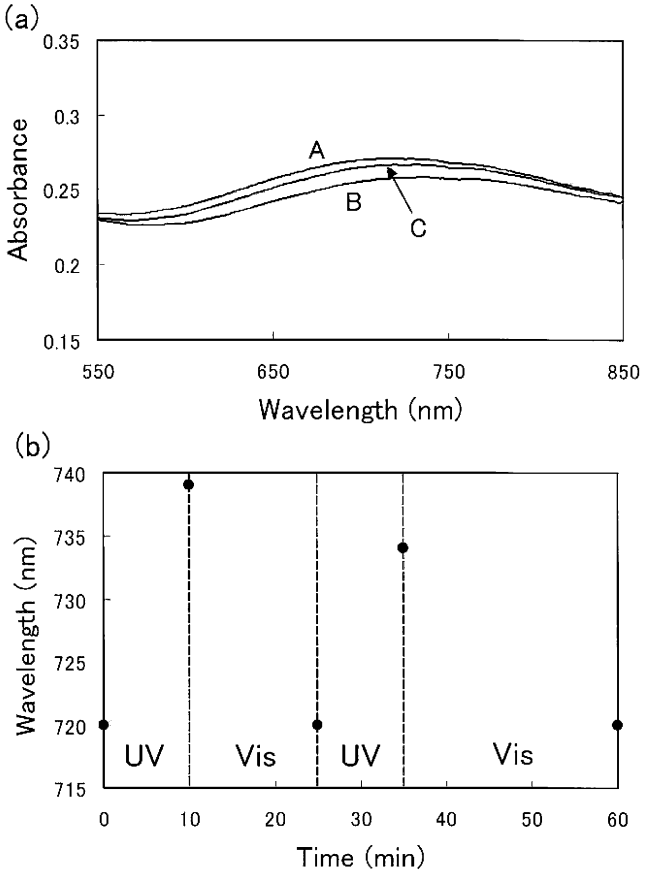

Figure 10. (a) Changes in the absorption spectra for a 100-layer hybrid film in the region of the IVCT band from Fe^{II} to Fe^{III} in the PB layer by alternate UV and visible light illumination. The initial trans state (A) was first illuminated with UV light for 20 min (B). Then, it was subsequently illuminated with visible light for 20 min (C). (b) Changes in λ_{max} (the IVCT band from Fe^{II} to Fe^{III} in the PB layer) by alternate UV and visible light illumination against photoillumination time.

As mentioned before, the absorption maximum, λ_{max} (the IVCT band from Fe^{II} to Fe^{III} in the PB layer) for the hybrid multilayered films was observed at around 700 nm. Figure 10a shows the changes in the λ_{max} before and after the alternating photoillumination. After UV illumination, the λ_{max} peak was red-shifted from 720 to 739 nm. On the other hand, after visible light illumina-

(50) Herren, F.; Fischer, P.; Lüdi, A.; Hälg, W. *Inorg. Chem.* **1980**, *19*, 956.

tion, the λ_{max} peak was blue-shifted from 739 to 720 nm. This reversible change was repeated several times in the area from curve B to C by alternately illuminating with UV and visible light. The wavelength of λ_{max} was plotted as a function of the illumination time in Figure 10b. This reversible change is almost consistent with the changes in the magnetization (Figure 9). By analogy with our previous system,[10] it is proposed that the photoisomerization of the azobenzene chromophore was accompanied by a geometrically confined structural change, as reflected by changes in the dipole moment and the electrostatic field.[9,10] Also, in the present system, changes in the electrostatic field driven by the photoisomerization of the azobenzene chromophore led to changes in the Coulombic energy, which is necessary to transfer an electron from the hexacyanoferrate(II) ion to Fe^{III} species, and this might affect the superexchange interaction between the spins in the PB magnet.

Review of System. We have succeeded in designing a photofunctional system whose magnetic properties can be controlled by photoillumination. This photoswitching of the magnetization was due to the formation of well-organized hybrid multilayered films that possess four remarkable features. First, the layered structure of the film was quite stable, due to the rigid clay layers. By introducing the clay layers into the system, the durability of the film was enhanced with respect to the structural changes induced by the photoisomerization. Second, we could prepare a stable monolayer containing $C_{12}AzoC_5N^+$ spread onto a subphase of the clay suspension. In general, $C_{12}AzoC_5N^+$ does not form a stable monolayer on pure water because of its relatively high water solubility. However, in the presence of the clay platelets, the $C_{12}AzoC_5N^+$ was hybridized with the clay, which prevented it from dissolving in the subphase. Third, we could intercalate the PB thin layers into the hybrid film as an adsorbed layer by an ion-exchange reaction with the clay layers. This method can be effective for introducing cationic compounds into the film as adsorbed layers. Therefore, it is expected that various kinds of functional films will be designed by adopting this procedure. Fourth, it is easy to control the density of the PB layers by changing the clay concentration in the suspension, because the cation-exchange capacity of the outer surface of the film depends on the concentration of the clay in the suspension. The density of the PB layers is also dependent on that of the $C_{12}AzoC_5N^+$ forming the hybrid films. In detail, the adsorption rate of PB is determined by the remaining cation-exchange capacity after the formation of the hybrid films. Therefore, the density of the PB layers is also controllable by varying the packing of the $C_{12}AzoC_5N^+$ in the transferred hybrid multilayered films. To increase the density of the PB layers, one may transfer the hybrid films at a lower surface pressure.

Conclusions

We have designed a new photofunctional LB film consisting of amphiphilic azobenzene cations, a smectite clay, and Prussian Blue, whose magnetic properties could be controlled by photoillumination. The present work demonstrates that an air−suspension interface can be quite effective for designing novel photofunctional systems due to its highly ordered structure. In addition, this strategy may offer new perspectives, not only for photofunctional materials but also for nanoscale composite materials.

Acknowledgment. This work was supported by a Giant-in-Aid for Scientific Research on Priority Areas (417) from the Ministry of Education, Culture, Sports, Science and Technology (MEXT) of the Japanese Government.

CM035223D